On the Series of +CG Lightning Strokes in Dancing Sprite Events

J. Bór1, Z. Zelkó2, T. Hegedüs2, Z. Jäger2, J. Mlynarczyk3, M. Popek4, and H. D. Betz5

1Research Centre for Astronomy and Earth Sciences, GGI, Hungarian Academy of Sciences, Sopron, Hungary

2Baja Observatory of the University of Szeged, Baja, Hungary

3AGH University of Science and Technology, Department of Electronics, Krakow, Poland

4Department of Space Physics, station Nýdek, Institute of Atmospheric Physics, CAS, Prague, Czech Republic

5Physics Department, University of Munich, and Nowcast GmbH, Munich, Germany

Corresponding author: József Bór (jbor@ggki.hu)

Key Points:

- The observations support that dancing sprite events tend to occur above stratiform cloud areas.
- If a sprite is up to 45 km away from its parent +CG stroke, the offset of the next sprite in the same sequence was found to be larger.
- It is suggested that +CG parent strokes in dancing sprite events are often part of one extensive lightning flash.

Keywords:

lightning, lightning dynamics, TLE, dancing sprites, leader propagation, thunderstorm, electric charge distribution, stratiform region, triangulation, current moment

Abstract

In dancing sprite events, sprite entities and groups appear in rapid succession together with a corresponding series of parent lightning strokes. Dancing sprite events, including a case with possible sprite re-brightening, were recorded on video simultaneously from two observation sites above a mesoscale convective system in Central Europe on the night of August 6, 2013. Joint analysis of triangulated locations of sprite elements, position, type and peak current of lightning strokes from the LINET lightning detection network database, and current moment waveforms deduced at the

Hylaty station, Poland, showed that subsequent sprite-parent lightning strokes occurred no further than 21 km from the closest preceding sprite entity in the cases analyzed in this study. Additionally, it was found that longer sprite delay times tend to correspond to larger sprite offsets from the parent +CG stroke. These observations, the occurrence of +CG lightning stroke and sprite sequences, and sprite-sprite offsets and displacements can be explained if +CG strokes are part of one extended lightning flash. A corresponding production mechanism based on previous findings on the formation of sprite-producing and general +CG lightning discharges is suggested.

Plain Language Summary

In dancing sprite events, sprites appear in rapid succession together with a corresponding series of parent lightning strokes. Dancing sprite events were recorded on video simultaneously from two observation sites above an extended thunderstorm system in Central Europe on the night of August 6, 2013. Comparison of triangulated sprite locations and the locations of corresponding lightning activity revealed that subsequent sprite-parent lightning strokes occurred below or relatively near to the location of the closest preceding sprite entity in the examined cases. In this paper, a mechanism is suggested for the development of lightning flashes which produce dancing sprites. The proposed mechanism accounts for prompt and delayed sprites relative to their parent lightning stroke, highlights the role of the variation of lightning current in sprite production, and it can explain the observed closeness of the next +CG lightning stroke to the area of previous sprites.

1 Introduction

Red sprites are one type of transient luminous events (TLE). They are brief luminous flashes accompanying electrical discharges in the mesosphere (Pasko et al., 2012). These high altitude electrical discharges are triggered by lightning processes of high vertical charge moment change (CMC) in the underlying thunderstorm (Hu et al., 2002). For cloud to ground (CG) lightning, vertical CMC is defined as the product of the amount of charge neutralized and the altitude of the charge center in the cloud.

Sprites are triggered most often by positive polarity (+CG type) lightning strokes (Lyons, 1996). Sprites triggered by cloud lightning (IC) (Neubert et al., 2005; Neubert et al., 2008) and negative polarity lightning strokes (Boggs et al., 2015; Lang et al., 2013) are reported much less frequently. The appearance of a sprite can be delayed with respect to its parent lightning stroke. While most sprite delay times are less than 100 ms, delays over 200 ms, have been reported, too (Li et al., 2008; Lu et al., 2013; Lyons et al., 2003; Mika et al., 2005; Sao-Sabbas et al., 2003; Soula et al., 2015). Generally, longer sprite delays were found in winter thunderstorms than in summer continental thunderstorms (Greenberg et al., 2007; Matsudo et al., 2009). The location of the sprite (i.e., its footprint projected onto the ground) is often displaced from the location of its parent lightning stroke (SP+CG). Most sprite displacements are less than 50 km (Lu et al., 2013; Lyons, 1996; Sao-Sabbas et al., 2003; Soula et al., 2010).

1.1 Sprite-parent +CG lightning strokes and the triggering of red sprites

Examination of the progression of lightning leaders during the development of SP+CG discharges helped interpreting both delay times and displacements of sprites. Lightning discharges start from an initiation point from where the lightning channel develops in a bi-directional fashion (Mazur, 2002; van der Velde et al., 2014). Negative leaders tend to branch as they advance fast so that an extensive and dense network of lightning channels can be developed within a positive cloud region (Lang et al., 2010; Lu et al., 2009). Positive leaders on the other end of the lightning channel progress relatively slowly (van der Velde & Montanya, 2013; van der Velde et al., 2014) and don't tend to branch much. Positive and negative potential wells in the cloud (Coleman et al., 2003) polarize the conductive lightning channel so that part of the channel network, which is embedded in the positive cloud region, will be negatively charged.

Regarding the configuration of charged regions in the thundercloud, results from numerical modeling indicate that the initiation of +CG flashes requires a stronger, positively charged region above a negative region (Tan et al., 2014). Such situation can easily occur in the mature stage of thunderstorms in their stratiform cloud region (Marshall et al., 2001; Rakov & Uman, 2003, chapter 3.3; Stolzenburg et al., 1994; Stolzenburg et al., 1998), where horizontally extensive charge layers keep descending and charged precipitation can weaken a lower negative layer (Marshall et al., 2009; Zhang et al., 2015). This is consistent with reports confirming that SP+CGs tend to occur in the late mature stage of mesoscale convective systems (MCS) with extensive stratiform regions (Lyons et al., 1998; Lyons et al., 2003).

When the positive end of the lightning channel gets attached to the ground and a return stroke (RS) occurs, the whole network of interconnected conductive channels is brought to ground potential. Right after this, a quasi-static electric (QE) field builds up between the upper portion of the lightning channel network and the (positive) lower ionosphere. If the channel network in the upper (positive) cloud layer is extensive and dense, ground potential is effectively elevated and the QE field above the clouds will exceed the critical breakdown level for a high altitude electrical discharge. Consequently, prompt or very short delayed sprites and/or a sprite halo is produced (Hu et al., 2007; Pasko et al., 2012; Williams et al., 2012). Note that in such cases, i.e., when an extensive and dense network of polarized lightning channels exists in the cloud before the RS, large amount of negative charge will be transported into the cloud during the RS. If, additionally, the channel network had been extended to high altitudes, the corresponding vertical CMC of the +CG stroke will be indeed large (Hu et al., 2002).

Sprites often appear above the area where negative leaders propagated just before the occurrence of SP+CG RS (Stanley, 2000). This is not surprising because the density of the lightning channels is the highest near the latest position of leader tips due to the frequent branching of negative leaders. Consequently, the induced QE field, too, is the strongest exactly there. That area is usually displaced from the location of the ground strike. Lu et al. (2013) found displacements of <30 km after SP+CGs with initial CMC in excess of +200 C•km. Such displacement can be expected since the faster propagating negative lightning leaders can travel larger distances compared to slower positive leaders (van der Velde & Montanya, 2013).

Should the amplitude of the QE field remain below the breakdown threshold, no sprite appears. Low QE field in the mesosphere may occur if the network of negatively charged lightning channels is not

well developed at the time of the RS and/or if that network is embedded in a lower positive layer of the thundercloud so it is farther down from the lower ionosphere.

Propagation of the negative leaders, nevertheless, continues after the return strokes (Lu et al., 2009). If continuing current in the SP+CG supports the extension of the network of negatively charged lightning channels further and beyond a point where the corresponding high altitude QE field exceeds the critical breakdown level in the mesosphere, red sprites will occur. Sprites produced this way will be delayed more from their parent +CG and, depending on the propagation direction of negative leaders, larger location offsets can be anticipated.

1.2 Dancing sprites

While sprite delays and offsets have been discussed for events that were associated with one SP+CG, these properties are less well explored in events including more SP+CGs, like, i.e., some of the so called 'dancing sprite' events. Sprite entities often appear in groups or clusters (Bór, 2013) covering an area of several tens of km2 (Mlynarczyk et al., 2015; Soula et al., 2014; Winckler et al., 1996). The term 'dancing' sprites (also called 'jumping' sprites) was first suggested by Lyons (1994) who observed several clusters of sprites flashing up one after the other above lightning discharges of length over 200 km in the USA. Since then, the proposed term refers to a special type of sprite clusters in which the elements or sub-clusters appear in a sequence with lateral offset between the successive appearances (Bór, 2013; Füllekrug et al., 2013; Hardman et al., 2000; Lang et al., 2011; Lu et al., 2013; Lyons, 1996; Mlynarczyk et al., 2015; Soula et al., 2017; Williams et al., 2010; Winckler et al., 1996; Yang et al., 2015). Reports on these events agree in that dancing sprite sequences with total durations of several hundred milliseconds occur above the stratiform region of mesoscale convective systems (MCS) and are often associated with extended lightning flashes spanning hundreds of kilometers which can include sequences of several +CG lightning strokes (Lang et al., 2010; Soula et al., 2010; Walter Lyons, personal communication).

Dancing sprites with short delayed (dt ≤20 ms) and long delayed (dt >20 ms) elements have been associated to parent lightning flashes which include several SP+CG lightning strokes (Winckler et al., 1996; Hardman et al., 2000; Füllekrug et al., 2013; Soula et al., 2017) or to single stroke lightning discharges with continuing current (CC) and superimposed current surges (Lu et al., 2013; Yang et al., 2015). The important role of in-cloud extension and progression of lightning leaders in the production of sprites delayed and displaced with respect to their parent lightning stroke has been emphasized (Lu et al., 2013; Soula et al., 2017). This finding is coherent with the observation that elements of a dancing sprite cluster appear often more or less aligned (Bór, 2013).

1.3 Motivation

This paper concentrates on case studies of dancing sprites associated with a sequence of SP+CG strokes. The studied events occurred in a vigorous thunderstorm in Central Europe and were observed simultaneously from two separate locations, so that location of sprite entities and clusters could be determined by optical triangulation. Although accurate localization of sprites enables reliable examination of the relationship between sprites and their parent lightning strokes, triangulated sprite locations were not utilized in many studies to this date due to the relative rarity of multi-site optical observations (Lu et al., 2013; Lyons, 1996; Mende et al., 2002; Mlynarczyk et al., 2015; Soula et al., 2015; Soula et al., 2010; Stenbaek-Nielsen et al., 2010; Wescott et al., 2001).

In this study, triangulated location and appearance time of dancing sprites are compared to the properties of the corresponding SP+CGs in order to find clues about the physical nature of possible connections between subsequent SP+CG lightning strokes. Considering the stochastic nature of lightning, it could be expected that sprite-producing lightning occurs quasi-randomly and is distributed quasi-evenly within the area of favored conditions. While this has been observed more or less for general sprite-producing lightning (Lyons, 1996; Sao-Sabbas et al., 2003), SP+CG lightning strokes in a dancing sprite event occur in a sequence, close to each other both in space and time. This suggests that these electrical discharges are somehow connected.

2 Instrumentation, Data, and Methods

2.1 Optical observations, pairing of events, and triangulation

The parent thunderstorm system of the studied events was observed simultaneously from two locations, Nydek (49.668°N, 18.769°E), Czech Republic and Sopron (47.6837°N, 16.5830°E), Hungary, separated by 273 km in Central Europe (Figure 1). Optical instrumentation at these sites will be summarized here only briefly because it was described in detail in earlier reports (Bór, 2013; Mlynarczyk et al., 2015). Watec 910Hx and Ultimate 902H2 cameras equipped with Computar F/1.0 and F/0.8 lens produced analogue video signal which was time stamped and digitized in 720×576 pixel resolution. The UFO Capture detection software was used to recognize and record the events realtime. De-interlacing the video frames resulted in 20 ms time resolution (50 video fields per second). The time source was internet time in Nydek and a local GPS antenna in Sopron, so that the detailed analysis in this study is relied only on the latter time information of millisecond accuracy.

Records of the same sprite events from the two sites were identified by the matching detection times and by the similarity of the optical appearances and dynamics of the emissions. At the selection of dancing sprite events, the definition given by Bór (2013) has been extended so that emissions were considered to be part of one dancing sprite event if the time delay between consecutive appearances was less than 500 ms and the location of the new sprites seemed to fit into the direction set out by the locations of previous emissions.

Azimuth of each sprite was calculated at the observation sites using spherical trigonometry. The intersection of sprite azimuths was then taken as the location the sprites, i.e., the coordinates of its footprint projected onto the surface of the Earth. The direction of the sprites was found with the help of the UFO Analyzer software by matching the stars in the video field with the star map as it appeared at each site at the given instance of time. The bottom of the bright sprite body or the topmost bead just below it (Bór, 2013) was used to find the direction of columniform sprites. In case of more extended shapes (e.g., carrots, angels (Bór, 2013)) and for sub-clusters of the event within which the sprite entities could not be distinguished well, the azimuths of the leftmost and rightmost edges of the bright emissions were determined at the height where the structure was the widest. Middle azimuths of these azimuth ranges were used to find the location of the center of the emissions and the width was then calculated using the distance of the center from the observation sites.

Uncertainty in deduced azimuths originates from the uncertainty of star map matching, from the finite spatial resolution of the images, and from the inaccuracy in selecting the corresponding pixels in extended emission parts. The combined effect of these factors resulted in +/- 0.075° and +/- 0.055° uncertainty of the deduced azimuths at Sopron and Nydek, respectively. The region of the analyzed events was 290-320 km away from Sopron and 250-270 km away from Nydek (Figure 1b). With the given geometry of the observation sites and the region of interest, the uncertainty range of the triangulated position of any point is less than 1 km.

2.2 Infrared (IR) satellite images

The movement of clouds in Central Europe was followed on images produced by the EISQ51 MSG satellite at 10.8 μm IR wavelength (Figure 1c-e). The images were accessible on the website www.sat24.com in a time resolution of 15 minutes. National borders are overlaid on the images but the parallax error due to the viewing angle and the varying height of the clouds is not corrected. No color scale was provided for the images but as a general rule, higher and colder cloud tops are whiter. Rapidly whitening and extending localized regions indicate areas of strong convection and uplift in which cloud tops reach high in the troposphere, cool down, and extend near the tropopause.

2.3 Lightning data

Information on the lightning strokes in the thunderstorm was obtained from the LINET lightning detection network (Betz et al., 2008, 2009). For each lightning stroke detected by its electromagnetic radiation in the VLF/LF band, LINET provides the GPS-based occurrence time in UTC with microsecond accuracy, the type of the stroke (CG or inter/intra cloud (IC)), location of the source within a few hundred meters in the vast majority of cases, estimated height of the source if it is an IC stroke, polarity and estimated peak current with an uncertainty of less than 10%.

2.4 Current moment (CM) variation and CMC estimates

East-west and north-south components of the atmospheric electromagnetic field are monitored in the 0.03-52 Hz range in the extremely low frequency (ELF) band at Hylaty station (49.204°N, 22.544°E) (Kulak et al., 2014) in Poland, ca. 700 km to the East from the region of interest (Figure 1a). CM variation in the source process is reconstructed by correcting the measured signals for transformations caused by the recording system and the propagation in the Earth-ionosphere spherical waveguide. Details of the method are discussed by Kulak et al. (2013), Mlynarczyk et al. (2015), and Mlynarczyk et al. (2017). Return strokes (RS) are characterized by their CMC obtained from the maximum recorded amplitude of the corresponding ELF signals using the impulse approximation (iCMC) (Berger et al., 1975; Kułak et al., 2010).

3 Observations

3.1 The parent thunderstorm of the studied sprites and the selection of events

Aligned to the movement of air masses in north-east direction, distinct centers of strong convection formed during the afternoon of 6 August, 2013 in Central Europe from eastern France and Switzerland across Germany to western Poland. By the evening, the cloud systems of the dominant

storms in Switzerland and Germany expanded and merged producing a large multi-core mesoscale convective system (MCS) covering more than 100.000 km2 (Figure 1c-e). Such lightning-active MCS are known to be efficient sprite producers (Lyons, 2006).

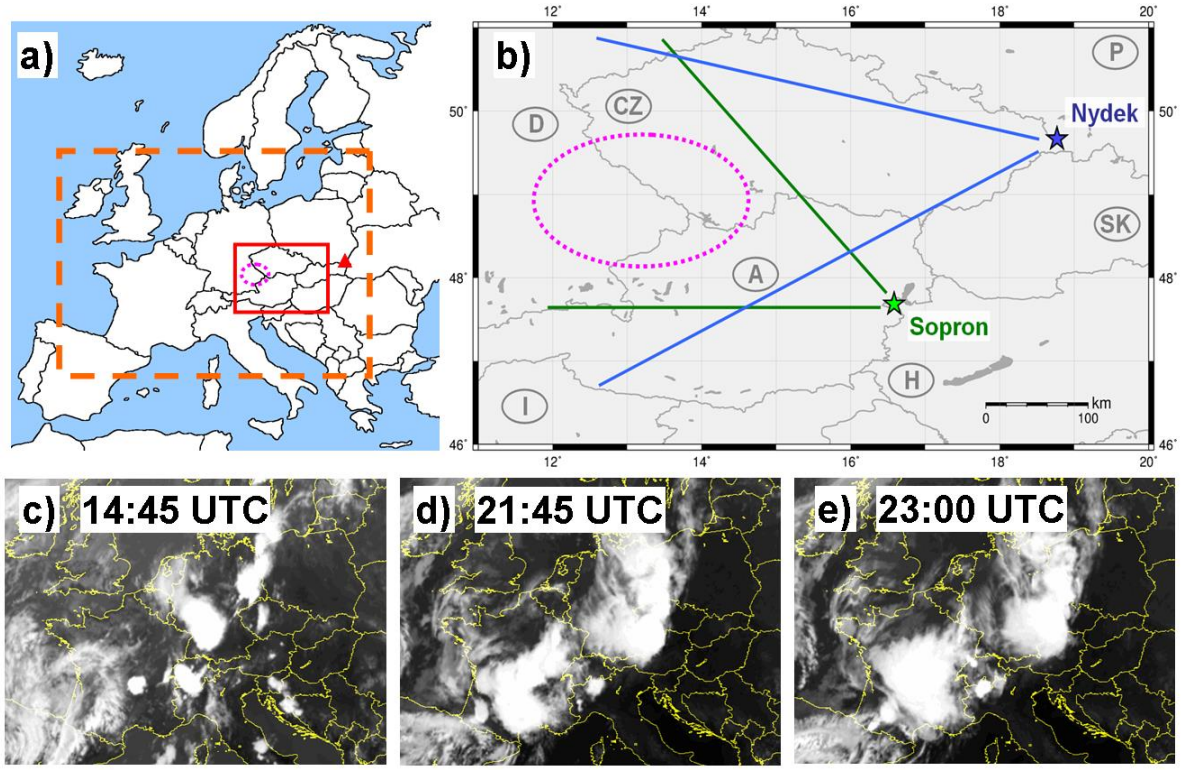

Figure 1. Overview of the region of interest. a) Overview map of Europe. Dashed line borders the area covered by the satellite images in panels c), d), e). Solid line borders the area shown in panel b). Dancing sprite events discussed in the paper occurred in the area marked by the dotted pink ellipse. The location of Hylaty ELF station is shown by the red triangle. b) Position of the region of interest, indicated by a dotted ellipse in pink, and the location of the observation sites in Sopron and in Nydek. The angle of the lines demonstrating the viewing angles is the actual angle used in the observations at each sites (45° and 37°, respectively). c)-e) Infrared satellite images of clouds covering Central Europe on 6 August, 2013.

During the night, mostly sprite events (a cluster of sprites was counted as one event as in Bór (2013)) and a few sprite halos were observed. 132 TLE were observed from Nydek between 19:37–02:00 UTC, and 68 from Sopron between 19:54–00:48 UTC. Out of the 32 events identified as dancing sprites, 17 were observed from both sites. This study is based on 5 cases, in which at least two SP+CGs were identified and the location of most sprite entities could be unambiguously triangulated. Four events were analyzed for the first time. The fifth dancing sprite event (from the same MCS) has been discussed in detail by Mlynarczyk et al., (2015). Out of the four recently analyzed cases, one characteristic example is discussed below in detail while other 3 events are described in detail in the supporting material.

3.2 The dancing sprite event at 23:06 UTC

This sequence of sprite emissions started with the appearance of two sprite entities at 23:06:20.008 UTC +/- 10 ms (Figure 2a, sprites A and B). The emissions faded on the next two video fields. Before

they completely vanished on the 5th field, the large carrot sprite C showed up on the 4th field and remained visible only for 2 video fields (up to 40 ms). After a pause of 180 ms (9 fields), sprites E and D appeared as a faint group of sprite beads (Bór, 2013) on the 15th video field. (Fields 6-14 are not shown in Figure 2a.) These sprites reached their final form during the next 4 video fields (80 ms), during which lower beads moved upwards, upper emission parts extended downwards and visually got interconnected. The emissions then faded and didn't survive more than 5 video fields. After another pause of 2 fields (40 ms), the elements of the final cluster of this event, sprites F,G, and H, appeared synchronously on field 22. All of these elements practically disappeared by the next video field, on which only very dim remnants of the streamer channels were visible in the records from Sopron.

By combining the information from triangulation (Figure 3d), lightning data (Table 1), and CM variation (Figure 4d) it can be concluded that the parent lightning stroke of sprites A and B (filled circles in Figure 3d) was a +CG lightning stroke with very high peak current (#1, 143.8 kA, pink cross in Figure 3d and 4d). The VLF/LF band waveform of the lightning sferic (not shown) indicates an unusual, double-pulse stroke. Despite of the high peak current, the iCMC of the stroke, 290 C•km, could not trigger mesospheric breakdown at once so that the sprites appeared after a short delay of up to 20 ms (one video field later). It must have been the strong CC following the +CG stroke (Figure 4d) which facilitated the production of the cluster of sprites A,B and, later, sprite C (Cummer & Füllekrug, 2001). Note that there are significant peaks in the current moment waveform which appear simultaneously with the appearances of these sprites. These peaks may represent either sprite currents (Cummer et al., 1998) and/or current enhancements superimposed on the CC like M components (Yashunin et al., 2007; Asano et al., 2009; Lu et al., 2016). Triangulation of the sprite locations shows that the later these sprites occurred the farther they were from their parent lightning stroke (Figure 3d).

The next sprite-producing lightning, a pair of +CGs (#2 and #3, 19.7 kA and 22.1 kA, respectively) occurred very close to each other and only 6-12 km away from the place where the last sprite (C) appeared (Figure 3d). It is possible that stroke #3 was a subsequent RS of stroke #2 (Saba et al., 2010). The forthcoming sprites (D and E) were a bit delayed as they occurred somewhat more than 23 ms later. Their appearance was accompanied by an enhancement in the CM upon the relatively slowly decaying CC that followed the strokes (Figure 4d). These sprites appeared at a distance of 36 km to the north-west from their parent lightning strokes. The next SP +CG (#4, 70.2 kA) occurred in the same direction 20 km away from the footprint of sprites D and E. This stroke had a relatively high iCMC of 590 C•km and it produced the final sprite cluster within 1 video field (20 ms) (Cummer & Lyons, 2005; Hu et al., 2002) with a horizontal offset of 10-20 km further in the W-NW direction.

Comparison of the spatial distribution of lightning strokes occurring in a +/- 10 min time window around the event (Figure 5d) and the movement of the cloud system (Figure 1c-e) shows that the dancing sprite event occurred most probably in the trailing stratiform region of the parent MCS. High density of lightning strokes indicates the location of uplift and deep convection (Keighton et al., 1991; Tuomi & Mäkelä, 2009; Yang et al., 2015). The first SP stroke was close to the center of lightning activity in the corresponding storm cell but occurred ca. 30 km downwind from it.

Figures 3, 4, and 5 include the corresponding results for other three dancing sprite events at 21:45 UTC, 22:13 UTC, and 22:42 UT from the same storm.

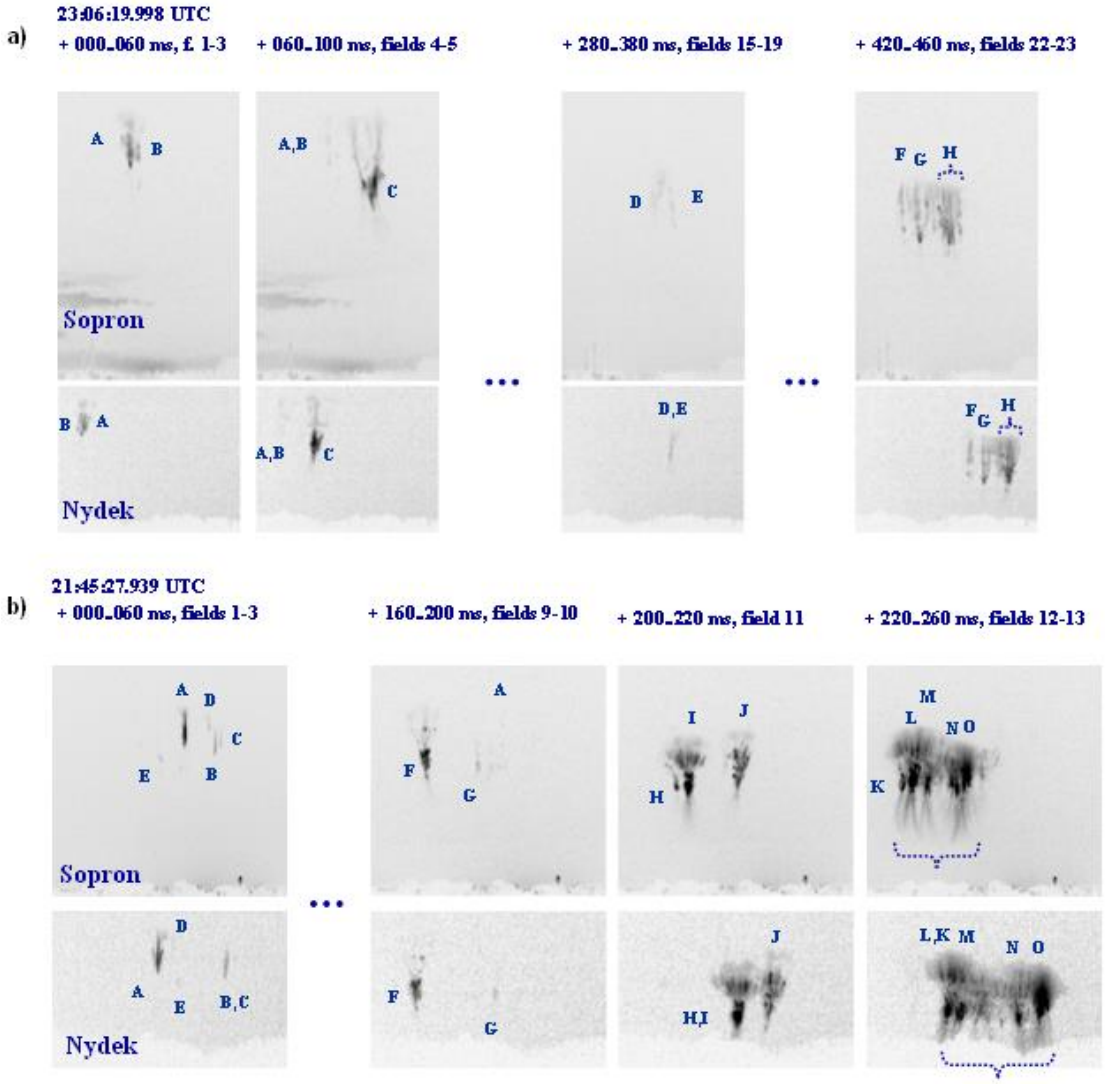

Figure 2. Sequence of inverted brightness peak-hold image pairs from videos recorded in Sopron and in Nydek. The images show sub-clusters of the dancing sprite event started at 23:06:20.008 UTC +/- 10 ms on 6 August, 2013. Before inversion, each pixel held its maximum brightness occurred during all video fields in the time interval displayed above the images. Time data correspond to the video from Sopron. The same number of video fields was processed to obtain the corresponding peak-hold image from Nydek but here the covered time interval is shifted by an unknown time interval of few ms. The full time string corresponds to the beginning of the exposition of the video field on which the first sprite emission was detected in Sopron. Time ranges (in ms) relative to this time point, absolute time intervals (seconds and ms only), and the serial number of corresponding video fields are given for each image pair. Triangulated sprite entities are noted by capital letters, triangulated sprite clusters are indicated by braces.

3.3 Offsets and delay times

Properties of SP+CG lightning strokes and triangulated sprites are summarized in Table 1. Note that stroke #1 in the event at 22:13 UTC is not counted in the statistics. This +CG did not trigger any sprite, however, the current moment analysis revealed that the sequence of +CGs associated to the

sprite event was in fact started with that stroke (Figure 4b). Additionally, only stroke #3 in the event at 23:06 UTC was used to calculate sprite offsets and delays.

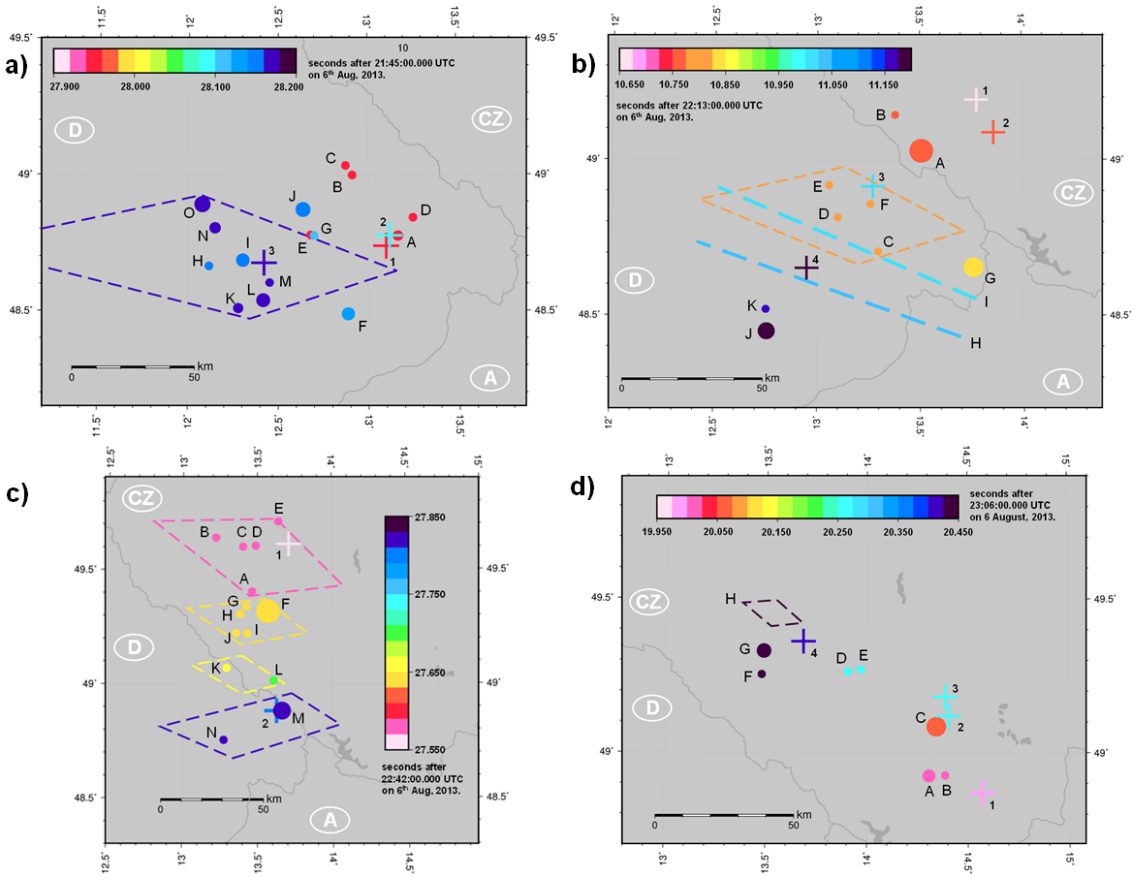

Figure 3. Dancing sprite events on 6 August, 2013. The location of triangulated sprite entities (filled circles), sprite clusters (the enclosing area is bordered by dashed lines), and sprite-producing lightning strokes (+) detected by LINET are shown. For carrot and angel sprites, the diameter of the filled circle is the actual width of the sprite body. In cases where a single point was triangulated and for columniform sprites, the size of the symbol does not represent the actual diameter of the source. (Sprite streamers have diameters only up to a few hundred meters (Marshall & Inan, 2006), so the symbol was enlarged to aid orientation.) The color of each symbol indicates the occurrence time of the corresponding sprite or lightning stroke. Capital letters identify sprites and numbers identify lightning strokes as listed in Table 1. a) Map for the event at 21:45 UTC. b) Map for the event at 22:13 UTC. Dashed lines indicate the direction of sprites H and I as these emissions were detected only from Sopron. Height information was not used to estimate the location; the lines were drawn across the area of sprite production. c) Map for the event at 22:42 UTC. d) Map for the event at 23:06 UTC.

Peak currents in the fourteen considered SP+CGs were in the range 17.4 – 143.8 kA. The average was 58 kA with only three values (21%) below 20 kA. The range of corresponding iCMC values was 105 – 2790 C•km so that the iCMC was between 300 and 900 C•km in 8 of 14 cases (57%). Two strokes had iCMC less than 300 C•km and four strokes had larger iCMC than 900 C•km. Note that only the cumulative iCMC could be determined for strokes #2 and #3 in the event at 23:06 UTC.

With stroke #2 in the event at 23:06 UTC counted in, 10 SP+CG strokes (71%) were subsequent strokes in sequences of SP+CGs. This result is consistent with the statistics reported by Soula et al. (2010). Distance of each subsequent SP+CG was considered from the closest localized sprite entity which appeared previously. Calculated SP+CG offsets from the closest previous sprite were within the range 3.4 – 20.7 km (Table 1). The offsets between successive +CGs within a dancing sprite event scattered between 4.5 km and 81.3 km. If strokes #2 and #3 in the event at 23:06 UTC are taken practically as one stroke, time delays between successive +CGs within a dancing sprite event are between 48 ms and 277 ms so that 7 of 10 delay times are well above 100 ms including 4 values above 200 ms (Table 1).

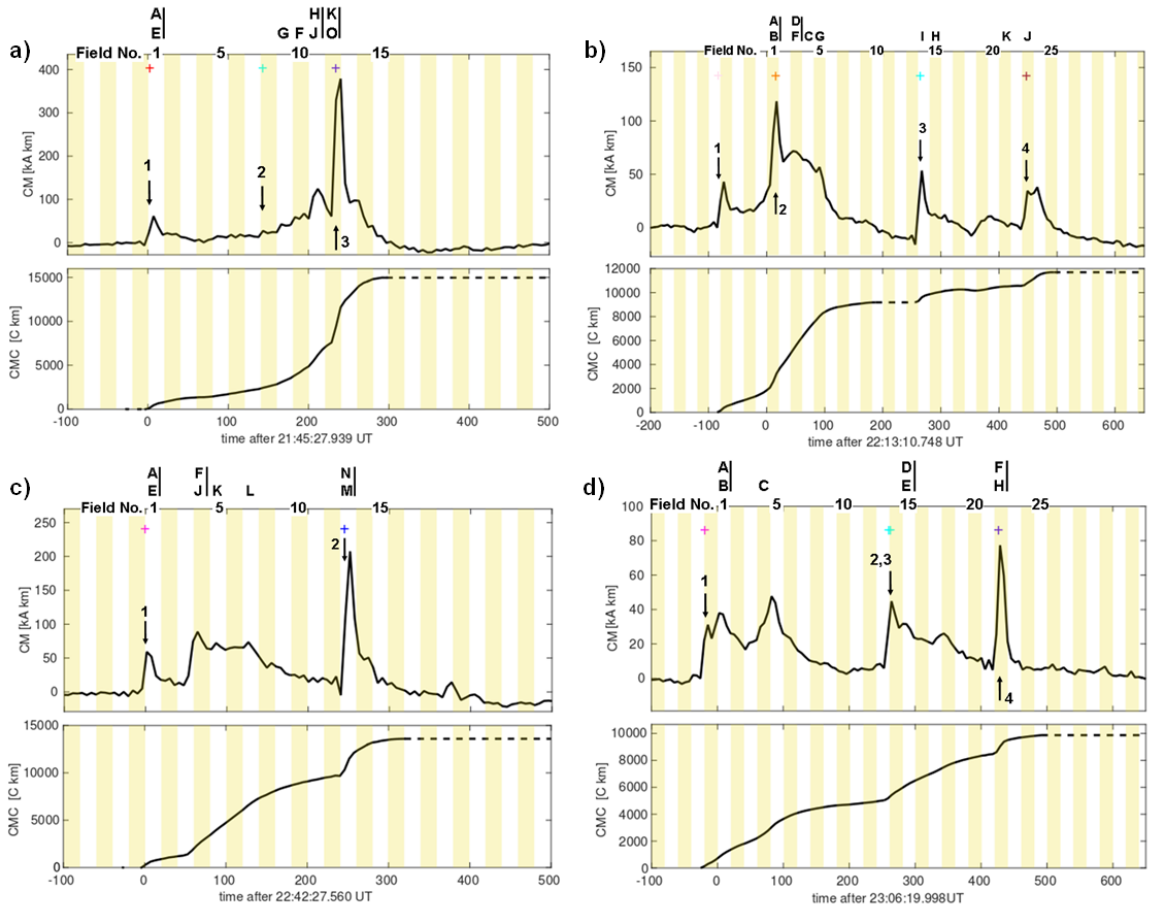

Figure 4. Variation of current moment (CM) and cumulated charge moment change (CMC) in the region of interest corresponding to dancing sprite events on 6 August, 2013. Time points of sprite-producing +CG lightning strokes identified by their serial numbers in Table 1 are shown by arrows and + signs. Serial numbers of video fields in Sopron with the letters of appearing sprites (Figure 3) are printed at the top of the panel. Only the first and the last letters are written alphabetically if several sprites appeared at the same time. a) Results for the event at 21:45 UTC. b) Results for the event at 22:13 UTC. c) Results for the event at 22:42 UTC. d) Results for the event at 23:06 UTC.

Appearance time of 47 sprite entities and 3 smaller sprite clusters (K and F in event at 22:34 and H in event at 23:06) was registered. From these, the location of 45 sprite entities and the 3 small clusters was determined by triangulation (Figure 3). Delay time of first sprites triggered by a SP+CG was less

than 20 ms in 8 of 14 cases (57%). The longest delay time of the first triggered sprite was 32 +/- 10 ms (sprites D and E in event at 23:06 UTC). The longest observed sprite delay in the complete set of events was 149 +/- 10 ms (sprite cluster K in event at 22:13 UTC) (Table 1).

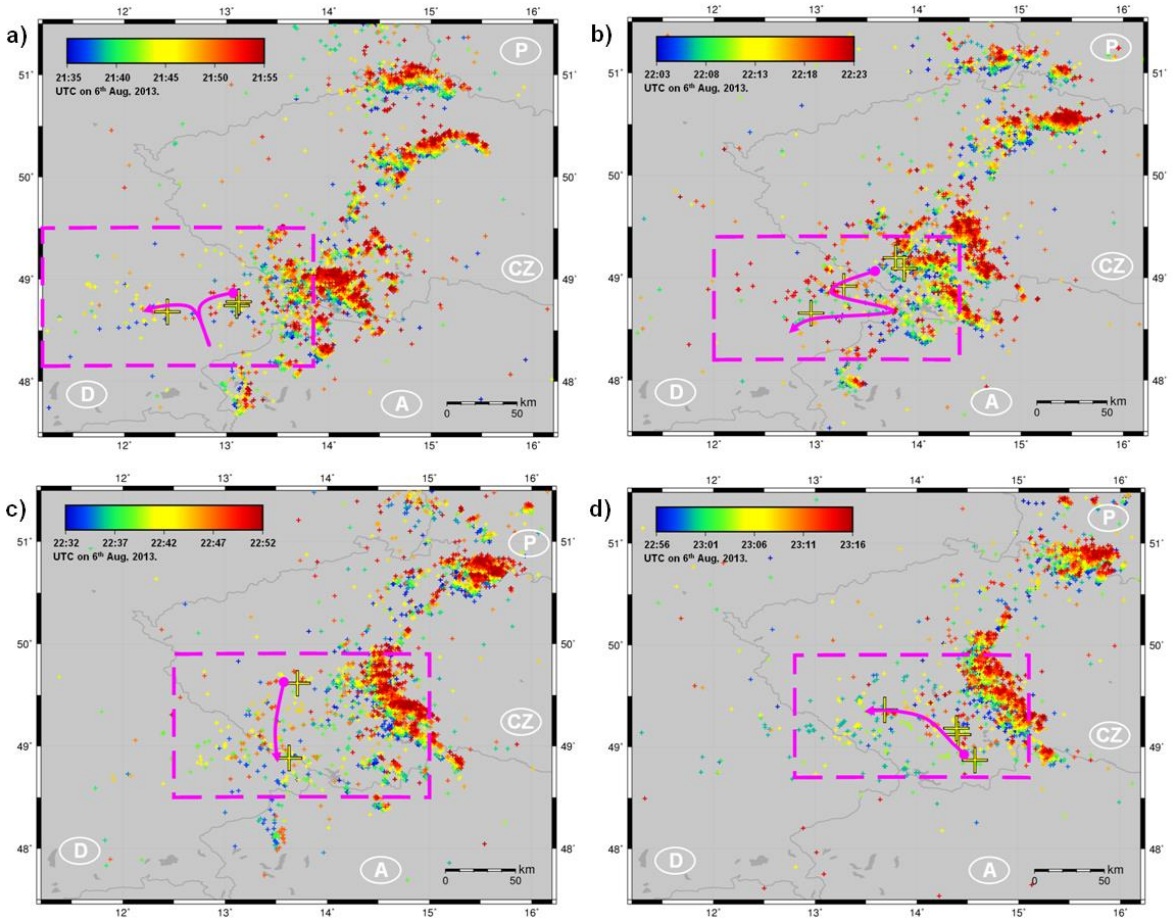

Figure 5. Overview maps of the region of interest shown in Figure 1b. The locations of lightning strokes of all types detected by LINET within a 10 minute interval around each event on 6 August, 2013 are marked by small + signs. SP+CG strokes are marked by large + signs. Time is color coded. Dashed line borders the area covered by the corresponding map in Figure 3. Note that a different map projection was used in this panel compared to that in Figure 3 to aid distinguishing the regions of high and low flash densities. The approximate center of the first sprite cluster is marked by a filled circle and the rough 'path' followed by the footprints of later appearing sprites is indicated by an arrow. a) Map for the event at 21:45 UTC. b) Map for the event at 22:13 UTC. c) Map for the event at 22:42 UTC. d) Map for the event at 23:06 UTC.

The displacement of sprite entities from their SP+CG varied in the range 2.6 – 74.7 km (Figure 6a). Sprites which appeared first after a SP+CG have characteristically smaller offsets (<~50 km) than later appearing sprites. This limiting offset value matches the one found by Soula et al. (2010) but is larger than the limit of 30 km reported by Lu et al. (2013) for short delayed sprites. Some short delayed sprite entities in our set of events had offsets larger than 30 km, e.g. sprites K and L in the event at 22:34 (Table 1). Note that the trend that delayed sprites have larger offsets was reported earlier by Lu et al. (2013).

SP+CG data						Sprite data				
#	Time (UTC)	Longitude (deg)	Latitude (deg)	Imax (kA)	iCMC (Ckm)	Last closest sprite ID	Distance from last closest sprite (km)		Delay from last SP+CG	Offset
	Sprite ID	Delay from SP+CG (ms)	Offset from SP+CG (km) avg, min-max	Closest previous sprite ID	Distance from that sprite (km) avg, min-max	Delay from that sprite (ms)	Virtual speed (km/s)			
	Event start time:	21:45:27.949 UTC +/- 10 ms, 6 August, 2013								
1	21:45:27.941	13.1001	48.7422	53.2	570	-	-		-	-
	A - E	9 ± 9	24.4, 6.3-36.7	-	-	-	-			
2	21:45:28.080	13.1198	48.7804	18.9	105	A (inside)	3.4		139	4.5
	G/E	29 ± 10	30.7	E	1.5 / 0	159 ± 19	8.4 - 10.7 / N.A.			
	F	49 ± 10	36.2	G	34.8	20 ± 20	870.0 <			
	H, I, J	69 ± 10	57.4, 36.8-74.7	G	29.0, 11.6 - 44.6	20 ± 20	(290.0 - 1115) <			
3	21:45:28.171	12.4213	48.6812	74.9	2970	I (inside)	8.7		91	52.4
	K - O	4 ± 4	20.8, 8.4-34.6	I or H	18.6, 14.2-25.3	20 ± 20	(355.0 - 632.5) <			
	Event start time:	22:13:10.758 UTC +/- 10 ms, 6 August, 2013								
1	22:13:10.667	13.7779	49.1958	38.9	393	-	-		-	-
2	22:13:10.759	13.8600	49.0905	45.4	797	-	-		92	13.1
	A, B	4.5 ± 4.5	31.0, 26.5-35.5	-	-	-	-			
	D, E, F	39 ± 10	58.4, 50.7-63.1	A	33.1, 26.2 - 38.0	34.5 ± 14.5	534.7 - 1900			
	C	59 ± 10	59.1	F	17.2	20 ± 20	430.0 <			
	G	79 ± 10	48.7	C	34.4	20 ± 20	860.0 <			
3	22:13:11.009	13.2704	48.9182	49.7	555	F (inside)	6.4		250	47.0
	I	9.5 ± 9.5	no location	-	-	-	-			
	H	29 ± 10	no location	-	-	-	-			
	K	149 ± 10	58.0	-	-	-	-			
4	22:13:11.191	12.9494	48.6559	42.0	322	K (inside)	20.7		182	37.4
	J	8.5 ± 8.5	26.7	K	7.8	41.5 ± 18.5	130.0 - 339.1			
	Event start time:	22:34:06.969 UTC +/- 10 ms, 6 August, 2013								
1	22:34:06.956	13.4445	48.3787	81.8	700	-	-		-	-
	B, C	13 ± 10	20.7, 14.1-27.3	-	-	-	-			
	D	53 ± 10	47.0	C	20.6	40 ± 20	343.3 - 1030			
	E	73 ± 10	56.7	D	16.7	20 ± 20	417.5 <			
	F	113 ± 10	67.7	E	17.9	40 ± 20	298.3 - 860.0			
	G	133 ± 10	70.1	F	10.0	20 ± 20	250.0 <			
11	22:34:07.218	13.6803	48.9166	37.7	500	E (outside)	13.5		262	62.2
	H, I, J	11 ± 10	38.7, 32.2-46.3	G	26.4, 22.0 - 28.8	140 ± 20	137.5 - 240.0			
20	22:34:07.266	13.3663	49.0167	17.4	900	G (inside)	4.7		48	25.2
	K, L	6.5 ± 6.5	48.3, 42.6-54.0	H	22.9, 18.5 - 27.2	43.5 ± 16.5	308.3 - 1007			
	M	23 ± 10	42.4	L	14.2	20 ± 20	355.0 <			
	Event start time:	22:42:27.570 UTC +/- 10 ms, 6 August, 2013								
1	22:42:27.559	13.7090	49.6152	66.8	550	-	-		-	-
	A - E	11 ± 10	22.8, 12.0-35.2	-	-	-	-			
	F - J	71 ± 10	42.1, 34.2-50.3	A	15.0, 7.9 - 21.7	60 ± 20	98.8 - 512.5			
	K	91 ± 10	67.4	J	17.5	20 ± 20	437.5 <			
	L	131 ± 10	66.8	K	23.7	60 ± 20	296.3 - 592.5			
2	22:42:27.806	13.6271	48.8850	126.2	1740	L (outside)	14.8		247	81.3
	M, N	7 ± 7	16.0, 2.6-29.4	L	26.6, 15.3 - 37.8	120 ± 20	109.3 - 378.0			
	Event start time:	23:06:20.008 UTC +/- 10 ms, 6 August, 2013								
1	23:06:19.977	14.5708	48.871	143.8	290	-	-		-	-
	A, B	31 ± 10	17.6, 14.9-20.3	-	-	-	-			
	C	91 ± 10	29.2	B	17.8	60 ± 20	222.5 - 445.0			
2	23:06:20.254	14.4060	49.1220	19.7	337	C (outside)	5.9		277	30.4
3	23:06:20.256	14.3893	49.1844	22.1		C (outside)	11.2		2	7.0
	D, E	32 ± 10	33.8, 30.7-36.8	C	35.8, 34.1 - 37.5	220 ± 20	142.0 - 187.5			
4	23:06:20.423	13.6845	49.3647	70.2	590	D (outside)	19.4		167	54.9
	F, G, H	7.5 ± 7.5	16.1, 14.6-19.1	D	32.1, 31.1 - 34.0	142.5 ± 17.5	194.4 - 272.0			

Table 1. Parameters of sprite-producing lightning strokes and corresponding sprites. Horizontal gray line separates sprites between which at least 20 ms delay (one de-interlaced video field) was observed. Sprites are identified by capital letters (Figure 3 and 4). Note that the sum of the iCMC of strokes #2 and #3 in the event at 23:06 UTC is given because the ELF signals from these strokes could not be separated. Sprite G in the event at 21.45 UTC is considered to be a re-brightened self of sprite E. The notation inside and outside at the ID of previous sprite indicates that the SP+CG occurred within or outside, respectively, the area covered by previously appeared sprite elements (Figure 3).

The relation of displacements and delay times could be examined for 6 SP+CG strokes which produced a sequence of sprites (Figure 6b). In general, larger sprite delay times from the SP+CG correspond to larger sprite displacements. This trend was found to be valid generally for offsets up to ca. 45 km. At offsets larger than about 45 km, displacements grow slower with the growing delay times and the trend is even reversed in several cases. If the location of the corresponding sprites are examined (Figure 3), it can be seen that the 'path' along which sprites appear seems to bend in those cases so that the strait line distance to the SP+CG does not get larger or it does in fact shrink.

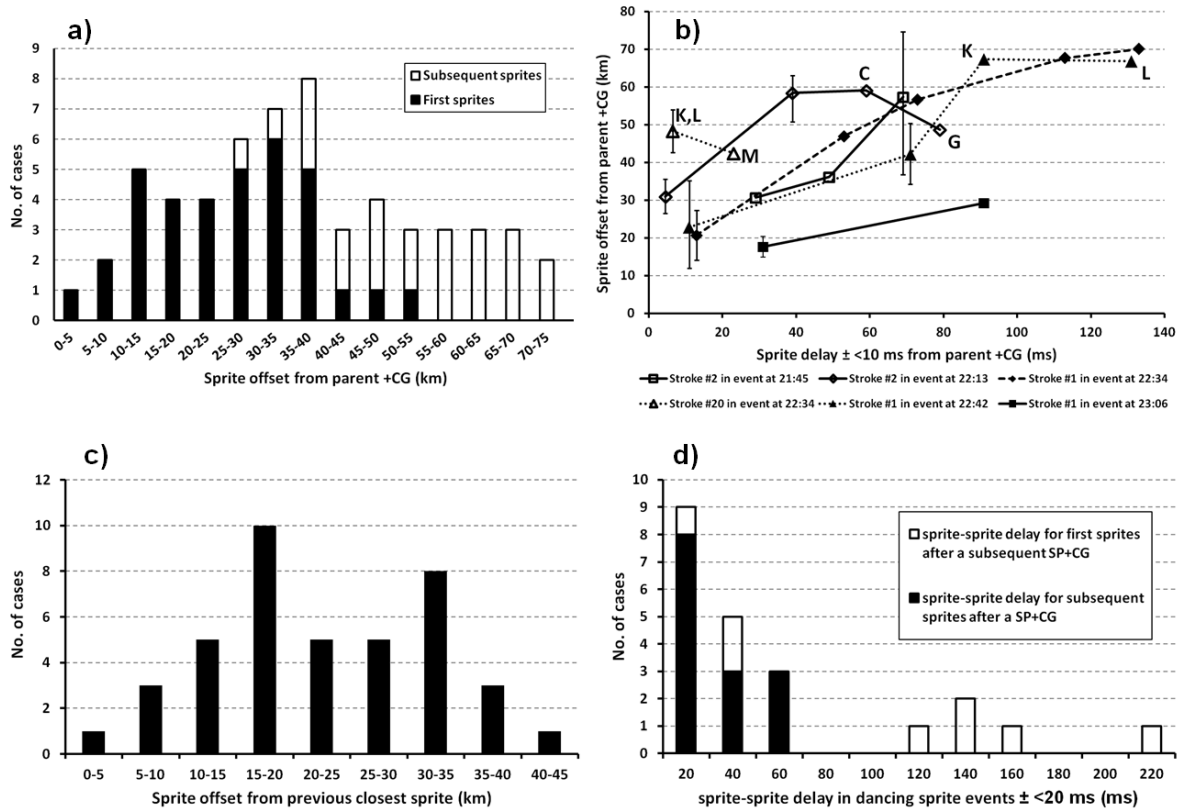

Figure 6. Delay times and displacements of sprites in dancing sprite events on 6 August, 2013. Plotted values are from Table 1. a) Histogram of sprite offsets from their parent +CG lightning stroke. Offsets of first sprites after parent +CG are distinguished from offsets of subsequent sprites. b) Relation of sprite offsets and delay times in cases when a sequence of sprite appearances were triggered by a single +CG lightning stroke. c) Histogram of sprite offsets from the closest sprite entity that appeared shortly before a sprite. d) Histogram of sprite delay times from the time point of preceding sprite appearance. Empty columns represent cases when a sprite-producing +CG stroke occurred between the two sprites.

The displacement between the subsequent sprite entities was also calculated. If more sprites have appeared on a single video frame previously, distance only to the closest one was considered. The sole exception to this rule was the group of sprites H, I, and J in the event at 21:45, where the distance was calculated not from the latest sprite (F) but from sprite G (Figure 3a). In that case, the liberty was taken to choose sprite G as reference because it was much closer to sprites H, I, and J than sprite F despite the fact that sprite F appeared after sprite G. Offsets of 41 sprites from the

closest previous sprite entity are shown in Figure 6c. According to this statistics, the majority of displacements between sprites and their closest previous sprite are in the 10 – 35 km range in the analyzed set of dancing sprite events with multiple SP+CG strokes.

Delay time of sprites from the previously appearing sprite within the same event has also been evaluated (Figure 6d). The distribution reveals that first sprites triggered by a subsequent stroke in a sequence of SP+CGs can have long (>100 ms) sprite-sprite delay times. All other subsequent sprites were delayed less than 80 ms from the preceding sprite.

3.4 Re-brightening of a sprite entity

In the event at 21:45 UTC, triangulated locations of sprites G and E agree within the 1 km uncertainty range for triangulation (Figure 3a). Sprite E appeared in the cluster triggered by the first SP+CG in the event. Compared to other sprites in the cluster, sprite E was a small-sized faint emission and it disappeared by the 4th video field (Figure 2a). Sprite G appeared only on the 9th video field as a faint patch 29 ± 10 ms after the second SP+CG in that sequence. The sprite showed explicit upward development on the next video field and remained visible even when the cluster with sprites H, I, and J appeared. These characteristics are very much similar to sprite re-brightening case documented by Füllekrug et al. (2013). These properties suggest that sprite G was a re-appearance of sprite E.

4 Discussion

4.1 Location of dancing sprites and the direction of their virtual movement in the parent thunderstorm

Dancing sprite events presented in this study occurred behind the convective cores of the parent thunderstorm system (Figure 5). This is consistent with previous experience that SP+CGs often occur behind (but close to) the convective cores of the thunderstorm (Carey et al., 2005; Lang et al., 2011; Lu et al., 2009; Soula et al., 2015). This result is also consistent with other observations showing that sprites, including dancing sprite events, very often occur above the stratiform cloud area of the parent storm close to the region of secondary radar enhancement or bright band (Lang et al., 2010; Lyons, 1996; Soula et al., 2015; Soula et al., 2017; Soula et al., 2010; Yang et al., 2015). Without available radar data, the location of stratiform cloud region could be estimated in this study only roughly from satellite IR cloud images (Figure 1), and from the distribution of lightning activity (Figure 5). The distance of stratiform region from the convective zone (characterized by dense lightning (Keighton et al., 1991; Tuomi & Mäkelä, 2009)) can be assumed to be about 25-50 km (Stolzenburg et al., 1998). Based on this, the event at 22:13 UTC is most probably an example for the well discussed scenario (Lang et al., 2010; van der Velde et al., 2014) in which the SP lightning is initiated in or close to a convective core while the corresponding network of lightning leaders extends downwind into the stratiform area (Figure 5b). The situation was similar for events at 21:45 UTC and 23:06 UTC, in which the first SP+CG occurred 30-40 km downwind from the convective cores (Figure 5a and 5d).

Regarding the events at 22:34 UTC and 22:42 UTC, the first SP+CGs were more than 50 km away from the nearest area of dense lightning so most probably the whole lightning process was embedded in the stratiform cloud region. It has been reported that the complete lightning process can take place fully within the stratiform region (Lang et al., 2010; Lu et al., 2013).

The direction in which lightning and sprite sequences virtually propagated was various across the stratiform cloud region but the direction tended to point away from the convective regions (Figure 5). Propagation of the lightning discharge is primarily determined by the propagation of negative leaders (Lang et al., 2017; Mazur, 2002). Negative leaders generally move in the direction of the largest positive potential gradient. Even if convective cores with upper positive charge centers (MacGorman & Rust, 1998, chapter 3.4) are close to the initiation point of the lightning discharge, negative leaders can escape the convective region and aim rather at the stratiform area. This was shown by lightning channel mapping (Lang et al., 2010; van der Velde et al., 2014) and also the observed propagation directions of sprite and +CG stroke sequences suggests this in dancing sprite events (Figure 5). This observation implies that positive potential in the stratiform cloud region can be very high due to the large amount of positive charge (Marshall & Rust, 1993) generated locally and transported there from the convective cores via advection in the ascending front-to-rare flow (Stolzenburg et al., 1994; Stolzenburg et al., 1998).

4.2 The sequence of SP+CG strokes in dancing sprite events

The usual time interval between common sprite events is on the order of minutes in sprite-producing periods of thunderstorms (Greenberg et al., 2007; Lyons, 1996; Lu et al., 2013; Neubert et al., 2008). The time interval between successive SP+CG strokes in dancing sprite events is only up to few 100 ms (Table 1). This short stroke interval, the spatial closeness of subsequent stroke, and the oriented fashion of the sequence suggest that these strokes are not independent from each other. Time intervals between SP+CG strokes in dancing sprite events are in the same range as those for +CG strokes associated to single very long lightning discharges (Lang et al., 2017; Lu et al., 2013; Soula et al., 2017; Soula et al., 2010). It is plausible to hypothesize that SP+CG strokes in many dancing sprite events are part of one long lightning discharge process. This scenario has been assumed also by Soula et al. (2010) for general sequences of CG discharges. This hypothesis can be verified unambiguously only by simultaneous optical observations and lightning channel mapping. The latter type of data is not available for the events studied in this work. Presented observations, therefore, cannot justify the hypothesis, but they at least support it in the following way.

As it was reviewed in the introduction, sprites appear above the area which was just previously explored by branching negative lightning leaders (Lu et al., 2013). If several sprites are produced by an extending lightning leader network, offsets between sequentially appearing sprites must match the propagation speed of negative lightning leaders. The propagation speed of negative lightning leaders in +CG discharges varies significantly from few 10 km/s to few 100 km/s and can be as high as 1000 km/s (van der Velde & Montanya, 2013). Whenever a subsequent SP+CG discharge occurred between successive sprites in the analyzed dancing sprite events, minimum virtual sprite speeds were in the range 8.4 – 1007 km/s (Table 1) which matches well with the experimentally measured negative leader speeds. But this is true also for other previous and following sprite pairs where minimum virtual speeds were within in the 130 – 1900 km/s range (Table 1) with most values falling between 100 km/s and 1000 km/s. Note that Soula et al. (2010) found similar virtual speeds for +CG stroke sequences.

A plausible resolution for the exceptionally low virtual speed (<100 km/s) between sprites G and E in the event at 21:45 UTC (Table 1) is that sprite G was not a new sprite but a re-brightening of sprite E after SP+CG stroke #2. If the offset and delay time of sprite G from its SP+CG stroke is taken, the

corresponding minimum speed is in the range 769.2 – 1616 km/s. This speed fits well to the value >870.0 km/s calculated between sprite G and the next sprite F.

Note that the calculated virtual speeds are lower bounds to the true values because strait line distances were taken between the sprites while negative leader paths are rather tortuous. The range of calculated virtual speeds is rather wide also because of the relatively high uncertainty in the appearance time of sprites (up to 40 ms, Table 1). When two events appeared on consecutive video fields, the higher value of the speed range could not be estimated since zero time difference could theoretically occur. Another assumption was that only one main lightning channel was considered, but bifurcation and branching of the main lightning channel can occur and in fact such cases have been reported (Lu et al., 2013; van der Velde et al., 2014).

In the analyzed cases, the next SP lightning stroke occurred systematically either within or close (< 21 km) to the area above which the preceding sprites appeared (Figure 3). Formation of these stroke sequences and their relation to previous sprite events can be speculated as follows by considering current knowledge on the evolution of lightning channels.

It has been shown that negative leaders can propagate several km for a few hundreds of ms after the main lightning channel to the ground is terminated (Lu et al., 2009). When the ground channel terminates, the network of lightning channels, being isolated from the ground, will be polarized again by the positive and negative potential wells in the cloud so that new positive leaders can start from the rear (positive) part of the channel network (Mazur, 2002). This mechanism explains the occurrence of subsequent +CG strokes close to a previous +CG stroke as SP+CG #2 in the event at 21:45 UTC.

As they grow long, lightning channels can become unstable (Heckman, 1992). Forward (active) section can be cut off from the mature (unstable) part of the channel network (Mazur, 2002). Positive leader development can then start from the rear section of the active leader channel and it can produce a new +CG return stroke more displaced from the previous one.

The location of the cutoff can be anywhere along the channel. Let us consider the case when the cut off active part of the leader network includes the area above which the latest sprites have been produced. As negative leaders propagate further away, this part of the channel network can become positive because of the polarization of the lightning channel. Positive potential will be the largest in this region because of the high density of lightning channels. Note that the high density of lightning channels had made it possible for sprites to occur above the same region previously. The newly acquired positive potential can facilitate the development of positive leaders so that the next +CG RS can occur below or very close to this region, i.e., the region of previously appearing sprites. The relative position of sprites and SP+CG stroke in the analyzed events (Figure 3) can be explained by this concept. The verification of the idea, however, requires more observations including lightning channel mapping.

Note that in the concept outlined above, the displacements of first sprites from their SP+CG depend on the differences in the speeds and propagation directions of positive and negative leaders before the RS happens. The maximum offset of delayed sprite depends on how long continuing current can support the propagation of negative leaders further. Cutoff of the forward negative channel limits

the growth of sprite offsets. Nevertheless, this study suggests that long contiguous lightning channels over 70 km may exist (Figure 6a).

4.3 Electrical discharging of the stratiform precipitation region

Until negative leaders can propagate in the cloud, the processes described above can be repeated and the sequence of +CGs can continue. Any new +CG stroke can trigger subsequent sprites if the network of negative leader channels in the forward section of the flash is dense enough and is at a sufficiently high altitude. Extensive and comprehensive discharging of the stratiform region, however, has not been observed at one go despite the accumulated large amount of charge (Marshall & Rust, 1993) and the presence of extensive as well as persisting horizontal charge layers (Marshall et al., 2001; Rakov & Uman, 2003, chapter 3.3; Stolzenburg et al., 1994; Stolzenburg et al., 1998). Although extremely long lightning flashes can be observed occasionally (Lang et al., 2017), the events in this study demonstrate that +CG sequences don't occur very often, generally last no longer than a few 100 ms, tend to propagate in some direction, and have a finite length (less than 200 km in the cases presented here). What stops the propagation of negative leaders?

This question has not been answered yet to the knowledge of the authors. We suggest that uneven distribution of positive charge in the stratiform region of thunderstorms can possibly be one part of the answer. Lu et al. (2013) confirmed sprite-associated charge removal from the cloud from a circular region with a diameter of few km. Additionally, in situ measurements made by aircrafts revealed that ~10 km scale horizontal variations of large amplitude are present in the electric field across the stratiform region (Mo et al., 2003).

It is plausible to postulate that it is the distribution of positive charge and the actual potential difference in front of negative leader tips which primarily determines the development of the lightning flash (Tom Warner, personal communication). If negative leaders are not supported by continuing current and they reach a region that has a lower positive potential as, for instance, it had been discharged earlier, the potential difference in front of the leader tip will not be sufficient to support further propagation and the discharge stops. On the other hand, if negative leaders approach a region of higher charge density, the potential difference in front of the leader tips grows. Regions of larger charge density can attract negative leaders and can direct their propagation. Intense branching and faster propagation of negative leaders in the vicinity of such positive charge centers can cause intensification of return stroke currents, similar to lightning M components (Yashunin et al., 2007). High spatial and temporal resolution mapping of the charge distribution in thunderstorms is needed to justify this speculation.

5 Summary

Triangulated locations of 45 sprite entities and 3 small sprite clusters, lightning data, and CM variation were studied in 5 dancing sprite events occurred in a sprite-producing MCS in Central Europe during the night of 6 August, 2013. (4 of these were analyzed in the framework of this study and another was discussed by Mlynarczyk et al. (2015)). Observations and hypotheses made upon the combined analysis are summarized as follows.

- All sprites in the examined events were triggered by +CG lightning strokes. SP+CG peak currents were in the range 17.4 – 143.8 kA, while corresponding iCMC values were in the range 105 – 2790 C•km.

- Comparing sprite locations to the spatial distribution of lightning strokes suggests that the analyzed dancing sprite events occurred in the trailing stratiform region of the MCS (Figure 5).

- The sequence of SP+CG strokes and the corresponding sprites advanced more or less in a parallel fashion in different directions across the trailing stratiform region but generally away from the cores of deep convection (Figure 5).

- In 4 out of the 5 examined cases, SP+CG sequences included more than 2 strokes. Time intervals between successive SP+CGs within an event were in the range 48 – 277 ms (Table 1).

- Both short-delayed (≤20 ms) and long-delayed sprites could be observed in the sprite sequences. The longest observed sprite delay time was 149 ± 10 ms (Table 1).

- Displacements of sprite entities from their SP+CG fell in the range 2.6 – 74.7 km. First sprites produced by a SP+CG have characteristically smaller offsets than subsequently appearing sprites (Figure 6a). Larger offsets from the SP+CG stroke correspond to longer sprite delay time if the offset of the previous sprite is below ca. 45 km; otherwise this relation is not unambiguous (Figure 6b).

- Distances between subsequent sprites within the events were below 50 km so that 83% of the sprite entities were displaced from the previous sprite by 10 – 35 km (Figure 6c).

- The longest delay time between subsequent sprites within an event was 220 ± 20 ms. Sprite-sprite delay times above 100 ms occurred only for sprites which appeared first after a subsequent SP+CG stroke (Figure 6d).

- The speed deduced from the delay time and displacement of subsequent sprites roughly matches the propagation speed of negative leaders in lightning flashes. Based on this finding it was suggested that SP+CG strokes in many dancing sprite events (possibly in all cases discussed in this paper) are part of one extended electrical discharge process. The need for combined measurements of lightning channel mapping and multi-station optical observations is emphasized in order this hypothesis to be verified.

- Results from triangulation suggest that a case of sprite re-brightening was observed (entities E and G in the event at 21:45 UTC) (Figure 2b).

- In the examined cases, all subsequent SP+CG lightning stroke occurred closer than 21 km to the previously appeared sprite entity (Table 1, Figure 3). This finding can be explained by assuming that the forward section of the extending negative leader channel gets cut off so that it can include the region above which previous sprites had occurred. Justification of this hypothesis cannot be made upon the presently available data so future multi-instrumental observations of similar cases are suggested.

- Finally, consideration of a possibly uneven charge distribution in positive cloud layers is suggested in explaining the disruption of electrical discharge processes in the extensive stratiform

precipitation region. The need for measuring the charge distribution in thunderclouds in high temporal and spatial resolution is emphasized to resolve this puzzle.

Acknowledgments, Samples, and Data

The Authors thank Dr. Walter Lyons and Dr. Tom A. Warner for their support and useful comments. The Authors are grateful for the useful comments and suggestions provided by the reviewers of this paper. This work was supported by the National Research, Development and Innovation Office, Hungary-NKFIH, K115836. Contribution of J. Bór was supported by the János Bolyai Research Scholarship of the Hungarian Academy of Sciences (BO/00651/13/10h). M. Popek acknowledges support from the Grant Agency of the Czech Republic (grant 17-07027S), and by the Praemium Academiae award from the CAS. J. Mlynarczyk has been supported by the National Science Center, Poland, under grant 2015/19/B/ST10/01055. The Authors appreciate support of the COST Action CA15211, ELECTRONET, in facilitating scientific communication. Data used to produce the results shown in this study can be reached from the website*, or available upon request from the authors.

*http://www.ggki.hu/~jbor/supplementary/Bor_et_al_2018_JGR_Atmospheres/

References

Asano, T., Suzuki, T., Hiraki, Y., Mareev, E., Cho, M. G., & Hayakawa, M. (2009), Computer simulations on sprite initiation for realistic lightning models with higher-frequency surges, J. Geophys. Res., 114, A02310, doi:10.1029/2008JA013651

Berger, K., Anderson, R. B., & Kroninger, H. (1975), Parameters of lightning flashes, Electra, 80, 223 – 237.

Betz, H.-D., Schmidt, K., & Oettinger, W. P. (2008), LINET – An International VLF/LF Lightning Detection Network in Europe, In Betz, H.-D., Schumann, U., & Laroche P. (Eds.), Lightning: Principles, Instruments and Applications, pp. 115-140, Dordrecht (NL): Springer

Betz, H. D., Schmidt, K., Laroche, P., Blanchet, P., Oettinger, W. P., Defer, E., … Konarski, J. (2009), LINET—an international lightning detection network in Europe, Atmos. Res., 91 (2), 564-573, doi:10.1016/j.atmosres.2008.06.012

Boggs, L. D., Liu, N., Splitt, M., Lazarus, S., Glenn, C., Rassoul, H., & Cummer, S. A. (2015), An analysis of five negative sprite-parent discharges and their associated thunderstorm charge structures, J. Geophys. Res. Atmos., 120, doi:10.1002/2015JD024188

Bór, J. (2013), Optically perceptible characteristics of sprites observed in central Europe in 2007–2009, J. Atmos. Sol.-Terr. Phys., 92, 151–177, doi:10.1016/j.jastp.2012.10.008.

Carey, L. D., Murphy, M. J., McCormick, T. L., & Demetriades, N. W. S. (2005), Lightning location relative to storm structure in a leading-line, trailing-stratiform mesoscale convective system, J. Geophys. Res., 110, D03105, doi:10.1029/2003JD004371

Coleman, L. M., Marshall, T. C., Stolzenburg, M., Hamlin, T., Krehbiel, P. R., Rison, W., & Thomas, R. J. (2003), Effects of charge and electrostatic potential on lightning propagation, J. Geophys. Res., 108(D9), 4298, doi:10.1029/2002JD002718

Cummer, S.A., & Füllekrug, M. (2001), Unusually intense continuing current in lightning produces delayed mesospheric breakdown, Geoph. Res. Lett., Vol. 28 ,No. 3, pp. 495-498, doi:10.1029/2000GL012214

Cummer, S. A., Inan, U. S., Bell, T. F., & Barrington-Leigh, C. P. (1998), ELF radiation produced by electrical currents in sprites, Geophysical Research Letters, Vol. 25, p. 1281, doi:10.1029/98GL50937

Cummer, S. A., & Lyons, W. A. (2005), Implications of lightning charge moment changes for sprite initiation, J. Geophys. Res., 110, A04304, doi:10.1029/2004JA010812

Füllekrug, M., Mezentsev, A., Soula, S., van der Velde, O., & Evans, A. (2013), Illumination of mesospheric irregularity by lightning discharge, Geophys. Res. Lett., 40, 6411–6416, doi: 10.1002/2013GL058502

Füllekrug, M., Mezentsev, A., Soula, S., van der Velde, O., & Farges, T. (2013), Sprites in low-frequency radio noise, Geophys. Res. Lett., 40, 2395–2399, doi:10.1002/grl.50408

Greenberg, E., Price, C., Yair, Y., Ganot, M., Bór, J., & Sátori, G. (2007), ELF Transients associated with sprites and ELVES in Eastern Mediterranean winter thunderstorms, J. Atmos. Solar-Terrestr. Phys., Vol. 69, Issue 13, pp. 1569-1586, doi:10.1016/j.jastp.2007.06.002

Heckman, S. (1992), Why does a Lightning Flash have Multiple Strokes?, Ph.D. thesis, Massachusetts Institute of Technology

Hardman, S. F., Dowden, R. L., Brundell, J. B., Bahr, J. L., Kawasaki, Z., & Rodger, C. J. (2000), Sprite observations in the northern territory of Australia, J. Geophys. Res., 105 (D4), 4689–4697, doi: 10.1029/1999JD900325

Hu, W., Cummer, S. A., & Lyons, W. A. (2007), Testing sprite initiation theory using lightning measurements and modeled electromagnetic fields, J. Geophys. Res., 112, D13115, doi:10.1029/2006JD007939

Hu, W., Cummer, S. A., Lyons, W. A., & Nelson, T. E. (2002), Lightning charge moment changes for the initiation of sprites, Geophysical Research Letters, Vol. 29, No. 8, 1279, doi:10.1029/2001GL014593

Keighton, S.J., Bluestein, H.B., & Macgorman, D.R. (1991), The evolution of a severe mesoscale convective system: cloud-to- ground/lightning location and storm structure, Monthly Weather Review, Volume 119, Issue 7, pp. 1533-1556, doi:10.1175/1520-0493(1991)119<1533:TEOASM>2.0.CO;2

Kulak, A., Kubisz, J., Klucjasz, S., Michalec, A., Mlynarczyk, J., Nieckarz, Z., … Zieba, S. (2014), Extremely low frequency electromagnetic field measurements at the Hylaty station and methodology of signal analysis, Radio Sci., 49, 361–370, doi:10.1002/2014RS005400

Kulak, A., Mlynarczyk, J., & Kozakiewicz, J. (2013), An analytical model of ELF radiowave propagation in ground-ionosphere waveguides with a multilayered ground, IEEE Trans. Antennas Propag., 61(9), 4803–4809, doi:10.1109/TAP.2013.2268244

Kułak, A., Nieckarz, Z., & Zięba, S. (2010), Analytical description of ELF transients produced by cloud-to-ground lightning discharges, J. Geophys. Res., 115, D19104, doi:10.1029/2009JD013033

Lang, T. J., Cummer, S. A., Rutledge, S. A., & Lyons, W. A. (2013), The meteorology of negative cloud-to-ground lightning strokes with large charge moment changes: Implications for negative sprites, J. Geophys. Res. Atmos., 118, 7886–7896, doi:10.1002/jgrd.50595

Lang, T. J., Li, J., Lyons, W. A., Cummer, S. A., Rutledge, S. A., & MacGorman, D. R. (2011), Transient luminous events above two mesoscale convective systems: Charge moment change analysis, J. Geophys. Res., 116, A10306, doi:10.1029/2011JA016758

Lang, T. J., Lyons, W. A., Rutledge, S. A., Meyer, J. D., MacGorman, D. R., & Cummer, S. A. (2010), Transient luminous events above two mesoscale convective systems: Storm structure and evolution, J. Geophys. Res., 115, A00E22, doi:10.1029/2009JA014500

Lang, T. J., Pédeboy, S., Rison, W., Cerveny, R. S., Montanya, J., Chauzy, ... Krahenbuhl, D. S. (2017), WMO World Record Lightning Extremes, Bull. Am. Meteor. Soc., vol. 98., No. 6, pp. 1153–1168, doi: 10.1175/BAMS-D-16-0061.1

Li, J., Cummer, S. A., Lyons, W. A., & Nelson, T. E. (2008), Coordinated analysis of delayed sprites with high-speed images and remote electromagnetic fields, J. Geophys. Res., 113, D20206, doi:10.1029/2008JD010008

Lu, G., Cummer, S. A., Li, J., Han, F., Blakeslee, R. J., & Christian, H. J. (2009), Charge transfer and in-cloud structure of large-charge-moment positive lightning strokes in a mesoscale convective system, Geophys. Res. Lett., 36, L15805, doi:10.1029/2009GL038880

Lu, G., Cummer, S. A. Li, J., Zigoneanu, L., Lyons, W. A., Stanley, M. A., ... Samaras, T. (2013), Coordinated observations of sprites and in-cloud lightning flash structure, J. Geophys. Res. Atmos., 118, 6607–6632, doi:10.1002/jgrd.50459

Lu, G., Cummer, S. A., Tian, Y., Zhang, H., Lyu, F., Wang, T., … Lyons, W. A. (2016), Sprite produced by consecutive impulse charge transfers following a negative stroke: Observation and simulation, J. Geophys. Res. Atmos., 121, doi:10.1002/2015JD024644

Lyons, W. A. (1994), Characteristics of luminous structures in the stratosphere above thunderstorms a simaged by low-light video, Geophys. Res. Lett., 21(10), 875–878, doi:10.1029/94GL00560

Lyons, W. A. (1996), Sprite observations above the U.S. High Plains in relation to their parent thunderstorm systems, J. Geophys. Res., 101 (D23), 29,641–29,652, doi: 10.1029/96JD01866

Lyons, W. A. (2006), The meteorology of transient luminous events – an introduction and overview, In Füllekrug, M., Mareev, E. A., & Rycroft, M. J. (Eds.), Sprites, Elves and Intense Lightning Discharges, Vol. 225 of NATO Science Series II. Mathematics, physics and chemistry, pp. 19–56, Dordrecht, the Neatherlands: Springer Verlag, doi:10.1007/1-4020-4629-4_2

Lyons, W. A., Cummer, S. A., Stanley, M. A., Huffines, G. R., Wiens, K. C., & Nelson, T. E. (2008), Supercells and sprites, Bull. Am. Meteor. Soc., vol. 89., issue 8, pp. 1165–1174, doi: 10.1175/2008BAMS2439.1

Lyons, W. A., Nelson, T. E., Warner, T. A., Ballweber, A., Lueck, R., Lang, T. J., ... Young, C. (2014), Meteorological aspects of two modes of lightning-triggered upward lightning (LTUL) events in sprite-producing MCS, 5th Intl. Lightning Meteorology Conf., Tucson, AZ, 8 pp.

Lyons, W. A., Nelson, T. E., Williams, E. R., Cummer, S. A., & Stanley, M. A. (2003), Characteristics of Sprite-Producing Positive Cloud-to-Ground Lightning during the 19 July 2000 STEPS Mesoscale Convective Systems, Monthly Weather Review, Volume 131, No. 10 , pp. 2414–2427, doi:10.1175/1520-0493(2003)131<2417:COSPCL>2.0.CO;2

MacGorman, D. R., & and Rust, W. D. (1998), The electrical nature of storms, Oxford, New York: Oxford University Press

Matsudo, Y., Suzuki, T., Michimoto, K., Myokei, K., & Hayakawa, M. (2009), Comparison of time delays of sprites induced by winter lightning flashes in the Japan Sea with those in the Pacific Ocean, Journal of Atmospheric and Solar-Terrestrial Physics, Volume 71, Issue 1, Pages 101-111, doi:10.1016/j.jastp.2008.09.040

Marshall, R. A., & Inan, U. S. (2007), Possible direct cloud-to-ionosphere current evidenced by sprite-initiated secondary TLEs, Geophys. Res. Lett., 34, L05806, doi:10.1029/2006GL028511

Marshall, T.C., & Rust, W.D. (1993), Two types of vertical electrical structures in stratiform precipitation regions of mesoscale convective systems, Bull. Am. Meteor. Soc., vol. 74, issue 11., pp. 2159–70, doi:10.1175/1520-0477(1993)074<2159:TTOVES>2.0.CO;2

Marshall, T. C., Stolzenburg, M., Krehbiel, P. R., Lund, N. R., & Maggio, C. R. (2009), Electrical evolution during the decay stage of New Mexico thunderstorms, J. Geophys. Res., 114, D02209, doi:10.1029/2008JD010637

Marshall, T. C., Stolzenburg, M., Rust, W. D., Williams, E. R., & Boldi, R. (2001), Positive charge in the stratiform cloud of a mesoscale convective system, J. Geophys. Res., 106(D1), 1157–1163, doi:10.1029/2000JD900625

Mazur, V. (2002), Physical processes during development of lightning flashes, C. R. Physique, 3, pp. 1393–1409, doi:10.1016/S1631-0705(02)01412-3

Mende, S. B., Frey, H. U., Rairden, R. L., Su, H-T., Hsu, R-R., Allin, T. H., ... & Inan, U. S. (2002), Fine Structure of Sprites and Proposed Global Observations, In Wang, H. N., & Xu, R. L. (Eds.), Cospar Colloquium Series Volume 14:Solar-Terrestrial Magnetic Activity And Space Environment, pp. 287-293, Elsevier

Mika, Á., Haldoupis, C., Marshall, R. A., Neubert, T., & Inan, U. S. (2005), Subionospheric VLF signatures and their association with sprites observed during EuroSprite-2003, Journal of Atmospheric and Solar-Terrestrial Physics, Volume 67, Issue 16, Pages 1580-1597, doi:10.1016/j.jastp.2005.08.011

Mlynarczyk, J., Bór, J., Kulak, A., Popek, M., & Kubisz, J. (2015), An unusual sequence of sprites followed by a secondary TLE: An analysis of ELF radio measurements and optical observations, J. Geophys. Res. Space Physics, 120, doi:10.1002/2014JA020780.

Mlynarczyk, J., Kulak, A., & Salvador, J. (2017). The accuracy of radio direction finding in the extremely low frequency range. Radio Science, 52, 1245–1252, doi:10.1002/2017RS006370

Mo, Q., Detwiler, A. G., Hallett, J., & Black, R. (2003), Horizontal structure of the electric field in the stratiform region of an Oklahoma mesoscale convective system, J. Geophys. Res., 108(D7), 4225, doi:10.1029/2001JD001140

Neubert, T., Allin, T. H., Blanc, E., Farges, T., Haldoupis, C., Mika, A., ... & Rasmussen, I. L. (2005), Co-ordinated observations of transient luminous events during the EuroSprite2003 campaign, J. Atm. Solar-Terr. Phys., 67, 807-820, doi:10.1016/j.jastp.2005.02.004

Neubert, T., Rycroft, M., Farges, T., Blanc, E.,Chanrion, O., Arnone, E., ... & Crosby, N., Recent Results from Studies of Electric Discharges in the Mesosphere, Surv. Geophys. (2008) 29: 71., doi:10.1007/s10712-008-9043-1

Pasko, V. P., Yair, Y., & C.-L. Kuo (2012), Lightning related transient luminous events at high altitude in the Earth's atmosphere: Phenomenology, mechanisms, and effects, Space Sci. Rev., 168, 475–516, doi:10.1007/s11214-011-9813-9.

Rakov, V.A., & Uman, M.A. (2003), Lightning: Physics and Effects, Cambridge, United Kingdom: Cambridge Univ. Press

Saba, M. F., Schulz, W., Warner, T. A., Campos, L. Z. S., Schumann, C., Krider, E. P., … Orville, R. E. (2010), High-speed video observations of positive lightning flashes to ground, J. Geophys. Res., 115, D24201, doi:10.1029/2010JD014330

Sao-Sabbas, F.T., Sentman, D.D., Wescott, E.M., Pinto, O., Mendes, O., & Taylor, M.J. (2003), Statistical analysis of space-time relationships between sprites and lightning, Journal of Atmospheric and Solar-Terrestrial Physics, Volume 65, Issue 5, p. 525-535., 2003, doi:10.1016/S1364-6826(02)00326-7

Soula, S., Defer, E., Füllekrug, M., van der Velde, O., Montanya, J., Bousquet, O., … Pedeboy, S. (2015), Time and space correlation between sprites and their parent lightning flashes for a thunderstorm observed during the HyMeX campaign, J. Geophys. Res. Atmos., 120, 11,552–11,574, doi:10.1002/2015JD023894.

Soula, S., Iacovella, F., van der Velde, O., Montanyà, J., Füllekrug, M., Farges, T., … Martin, J.-M. (2014), Multi-instrumental analysis of large sprite events and their producing storm in southern France, Atmos. Res., 135, 415–431, doi:10.1016/j.atmosres.2012.10.004.

Soula, S., Mlynarczyk, J., Füllekrug, M., Pineda, N., Georgis, J.-F., van der Velde, O., … Fabró, F. (2017), Dancing sprites: Detailed analysis of two case studies, J. Geophys. Res. Atmos., 122, doi:10.1002/2016JD025548

Soula, S., van der Velde, O., Palmiéri, J., Chanrion, O., Neubert, T., Montanya, J., ... & Lointier, G. (2010), Characteristics and conditions of production of transient luminous events observed over a maritime storm, J. Geophys. Res., 115, D16118, doi:10.1029/2009JD012066

Stanley, M. A. (2000), Sprites and their parent discharges, Ph. D. Thesis, New Mexico Inst. of Mining and Technology

Stenbaek-Nielsen, H. C., Haaland, R., McHarg, M. G., Hensley, B. A., & Kanmae, T. (2010), Sprite initiation altitude measured by triangulation, J. Geophys. Res., 115, A00E12, doi:10.1029/2009JA014543

Stolzenburg, M., Marshall, T.C., Rust,W.D., & Smull, B.F. (1994), Horizontal distribution of electrical and meteorological conditions across the stratiformregion of a mesoscale convective system, Mon. Wea. Rev., 122: 1777–97, doi:10.1175/1520-0493(1994)122<1777:HDOEAM>2.0.CO;2

Stolzenburg, M., Rust, W. D., Smull, B. F., & Marshall, T. C. (1998), Electrical structure in thunderstorm convective regions: 1. Mesoscale convective systems, J. Geophys. Res., 103, 14,059–14,078., doi: 10.1029/97JD03546

Tan, Y., Tao, S., Liang, Z.,& Zhu, B. (2014), Numerical study on relationship between lightning types and distribution of space charge and electric potential, J. Geophys. Res. Atmos., 119, 1003–1014, doi:10.1002/2013JD019983

Tuomi, T.J., & Mäkelä, A. (2009), Flash Cells in Thunderstorms, In Betz, H.-D., Schumann, U., & Laroche, P. (Eds.), Lightning: Principles, Instruments and Applications, pp. 115-140, doi:10.1007/978-1-4020-9079-0_23

van der Velde, O. A., & Montanya, J. (2013), Asymmetries in bidirectional leader development of lightning flashes, J. Geophys. Res. Atmos., 118, 13,504–13,519, doi:10.1002/2013JD020257

van der Velde, O. A., Montanyà, J., Soula, S., Pineda, N., & Mlynarczyk, J. (2014), Bidirectional leader development in sprite-producing positive cloud-to-ground flashes: Origins and characteristics of positive and negative leaders, J. Geophys. Res. Atmos., 119, 12,755–12,779, doi:10.1002/2013JD021291

Wescott, E. M., Stenbaek-Nielsen, H. C., Sentman, D. D., Heavner, M. J., Moudry, D. R., & Sao-Sabbas, F. T. (2001), Triangulation of sprites, associated halos and their possible relation to causative lightning and micrometeors, J. Geophys. Res., 106(A6), 10467–10477, doi:10.1029/2000JA000182

Williams, E., Kuo, C.-L., Bór, J., Sátori, G., Newsome, R., Adachi, T., ... & Su, H.-T. (2012), Resolution of the sprite polarity paradox: The role of halos, Radio Science, 47, RS2002, doi:10.1029/2011RS004794

Williams, E. R., Lyons, W. A., Hobara, Y., Mushtak, V. C., Asencio, N., Boldi, R., … Yamashita, K. (2010), Ground-based detection of sprites and their parent lightning flashes over Africa during the 2006 AMMA campaign, Q. J. R. Meteorol. Soc., 136, 257–271, doi:10.1002/qj.489

Winckler, J.R., Lyons, W.A., Nelson, T.E., & Nemzek, R.J. (1996), New high-resolution ground-based studies of sprites, J. Geophys. Res., 101(D3), 6997–7004, doi:10.1029/95JD03443

Yang, J., Lu, G., Lee, L.-J., & Feng, G. (2015), Long-delayed bright dancing sprite with large Horizontal displacement from its parent flash, Journal of Atmospheric and Solar-Terrestrial Physics, 129, 1–5, doi: 10.1016/j.jastp.2015.04.001

Yashunin, S. A., Mareev, E. A., & Rakov, V. A. (2007), Are lightning M components capable of initiating sprites and sprite halos?, J. Geophys. Res.,112, D10109, doi:10.1029/2006JD007631

Zhang, T., Zhongkuo, Z., Yang, Z., Changxiong, W., Hai, Y., & Fangcong, Z. (2015), Electrical soundings in the decay stage of a thunderstorm in the Pingliang region, Atmospheric Research, Volumes 164–165, Pages 188–193, doi: 10.1016/j.atmosres.2015.05.008